Colloids and Surfaces A: Physicochem. Eng. Aspects 457 (2014) 307–317

Contents lists available at ScienceDirect

Colloids and Surfaces A: Physicochemical and Engineering Aspects

journal homepage: www.elsevier.com/locate/colsurfa

Competitive adsorption of the protein hydrophobin and an ionic surfactant: Parallel vs sequential adsorption and dilatational rheology

Rumyana D. Stanimirova[a], Krastanka G. Marinova[a], Krassimir D. Danov[a], Peter A. Kralchevsky[a,*], Elka S. Basheva[a], Simeon D. Stoyanov[b,c], Eddie G. Pelan[b]

[a] Department of Chemical Engineering, Faculty of Chemistry and Pharmacy, Sofia University, 1164 Sofia, Bulgaria
[b] Unilever Research & Development Vlaardingen, 3133 AT Vlaardingen, The Netherlands
[c] Laboratory of Physical Chemistry and Colloid Science, Wageningen University, 6703 HB Wageningen, The Netherlands

HIGHLIGHTS

- At parallel adsorption, HFBII is hydrophilized and SDS occupies the interface.
- At sequential adsorption, the pre-adsorbed HFBII cannot be washed out by SDS.
- The co-adsorption kinetics of protein and surfactant below the CMC is quantified.
- Dilatational elasticity of adsorption layers is determined by oscillating bubbles.
- Two types of behavior of elasticity, linear and non-monotonic, are identified.

GRAPHICAL ABSTRACT

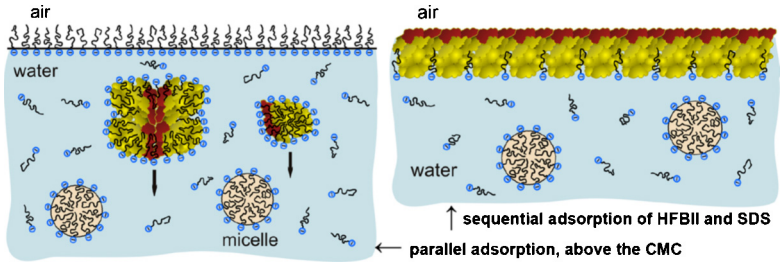

ARTICLE INFO

Article history:
Received 20 April 2014
Received in revised form 31 May 2014
Accepted 3 June 2014
Available online 10 June 2014

Keywords:
HFBII hydrophobin
Protein/surfactant co-adsorption
Dilatational surface rheology
Mixed adsorption layers
Protein displacement by surfactant

ABSTRACT

The competitive adsorption of the protein HFBII hydrophobin and the anionic surfactant sodium dodecyl sulfate (SDS) is investigated in experiments on parallel and sequential adsorption of the two components. The dynamic surface tension and the surface storage and loss dilatational moduli are determined by the oscillating bubble method. A new procedure for data processing is proposed, which allows one to collect data from many different runs on a single master curve and to determine more accurately the dependence of the dilatational elasticity on the surface pressure. Experiments on sequential adsorption are performed by exchanging the HFBII solution around the bubble with an SDS solution. Experiments with separate thin foam films bring additional information on the effect of added SDS. The results indicate that if HFBII has first adsorbed at the air/water interface, it cannot be displaced by SDS at any concentration, both below and above the critical micellization concentration (CMC). In the case of parallel adsorption, there is a considerable difference between the cases below and above the CMC. In the former case, SDS cannot prevent the adsorption of HFBII at the interface, whereas in the latter case adsorption of HFBII is absent, which can be explained with hydrophilization of the hydrophobin aggregates by the SDS in the bulk. The surface dilatational elasticity of the HFBII adsorption layers markedly decreases in the presence of SDS, but it recovers after washing out the SDS. With respect to their dilatational rheology, the investigated HFBII layers exhibit purely elastic behavior, the effect of dilatational viscosity being negligible. As a function of surface tension, the elasticity of the investigated interfacial layers exhibits a high maximum, which could be explained with the occurrence of a phase transition in the protein adsorption layer.

* Corresponding author. Tel.: +359 2 8161262; fax: +359 2 9625643.
E-mail address: pk@lcpe.uni-sofia.bg (P.A. Kralchevsky).

http://dx.doi.org/10.1016/j.colsurfa.2014.06.002
0927-7757/

1. Introduction

Hydrophobin HFBII is an amphiphilic protein produced by filamentous fungi [1]. Its adsorption layers at the air/water interface solidify fast. They possess elasticity, which is higher than that measured for all other investigated proteins [2–7]. The hydrophobin molecules are "sticky" – they adhere to each other, as well as to other macromolecules and solid walls. The hydrophobin is an excellent stabilizer of foams [8] and emulsions [9]; its adhesive properties lead to jamming in fluid dispersions [10]. The hydrophobins are used also for immobilizing functional molecules at surfaces [11], and as coating agents for surface modification [12].

Hydrophobins are relatively small and stable protein molecules. HFBII (70 amino acids) is rich in cysteine and is interconnected with four disulfide bonds. The hydrophobins are very hard to denature – their aqueous solutions have been heated to 90 °C without any sign of protein denaturing [1,13]. There may be some minor changes in shape for hydrophobins when they self-assemble, but this should not be confused with denaturing [1]. There are no evidences for denaturing of hydrophobins by surfactants.

The investigations of foam films stabilized with HFBII showed the formation of self-assembled hydrophobin bilayers due to the strong cohesion of the HFBII monolayers on the two film surfaces [14,15]. The adsorption kinetics and the dilatational rheology of HFBII interfacial layers have been studied by compression–expansion cycles in a Langmuir trough [16], and with oscillating drops [3], and an exceptionally high dilatational elasticity was measured. Very high shear elasticity has been determined for HFBII adsorption layers and interpreted in the framework of an appropriate rheological model [4,5]. The self-assembly of HFBII/surfactant complexes in the bulk of aqueous solutions and the adsorption behavior of HFBII/surfactant mixtures at the air/solution interfaces were investigated by neutron reflectivity and small-angle neutron scattering [17,18]. At surfactant concentrations below the CMC, the formation of mixed protein/surfactant adsorption layers was detected. However, the effect of surfactants on the dilatational surface rheology of hydrophobin adsorption layers has not been investigated so far. This is important for the stability and rheology of the foams and emulsions produced from the respective mixed solutions [2,7–10].

Our goal in the present study is to investigate the effect of sodium dodecyl sulfate (SDS) (i) on the kinetics of adsorption from mixed solutions with HFBII, and (ii) on the dilatational rheology, as well as (iii) to compare the properties of interfacial layers formed by parallel vs. sequential protein/surfactant adsorption.

In many studies [19–24], it has been established that at sufficiently high concentrations the surfactants are able to displace proteins, such as β-casein, β-lactoglobulin (BLG) and bovine serum albumin (BSA), from liquid interfaces. Experiments on dilatational surface rheology, including measurements with oscillating bubbles and drops [25,26], represent a sensitive method for the investigation of protein–surfactant interactions [27,28]. Two approaches to the realization of sequential adsorption with drops and bubbles have been realized: (i) exchange of the solution *inside* the drop by using coaxial capillaries [29,30] and (ii) exchange of the phase *outside* the bubble/drop by pumping out the old solution with a simultaneous supply of a new one [31,32]. Theoretical models of the kinetics of adsorption from mixed protein/surfactant solutions have been also proposed [33].

In Section 3, the kinetics of co-adsorption of HFBII and SDS is studied by experiments with buoyant bubbles. The measured surface-tension relaxation is quantitatively interpreted. In Sections 4 and 5, parallel and sequential adsorption of HFBII and SDS is investigated using phase exchanges. At different stages of the experiments, the surface dilatational moduli are measured by oscillatory experiments. Experiments with thin foam films are also carried out to confirm the conclusions from the rheological measurements. The HFBII/SDS system is compared with the BLG/SDS and BSA/SDS systems under similar experimental conditions. In Section 6, the dependencies of the dilatational elasticity of HFBII layers on the surface tension in the presence or absence of SDS are compared and discussed. A physical picture of the interfacial processes, which govern the surface pressure and elasticity, emerges from the analysis of the experimental data.

2. Materials and methods

2.1. Materials

In our experiments, we used class II hydrophobin (HFBII) of molecular weight 7.2 kDa isolated from the fungus *Trichoderma reesei* following a procedure described elsewhere [14]. Aqueous solutions with concentration 0.001 wt% (0.01 g/L) were used with a natural pH = 5.6. This relatively low protein concentration was selected on the basis of our previous experiments [3], which showed that at 0.001 wt% the HFBII adsorption layer at the air/water interface is relatively diluted and does not solidify. This is necessary, because we are using the oscillatory bubble method (OBM), which is applicable only to fluid interfaces. Indeed, in OBM the surface tension is determined by fitting the bubble profile with the Laplace equation. However, the profile of bubbles with solidified surfaces (with nonzero surface shear elasticity) could significantly deviate from the Laplacian shape, which would make the OBM inapplicable.

In comparative experiments, we used bovine serum albumin (BSA) – a globular protein of molecular weight 66.4 kDa, composed of 580 amino acid residues with 17 disulfide bonds (product of Sigma, A7511). The other used protein was β-lactoglobulin (BLG, Sigma, L0130) – a milk protein of molecular weight 18.4 kDa, composed of 162 amino acid residues with 2 disulfide bonds. Aqueous solutions of concentration 0.01 wt% were prepared and used overnight. Their natural pH was 6.1 ± 0.1. Sodium dodecyl sulfate (SDS, product of Acros Organics, Pittsburgh, PA) was used at concentrations varying from 1 to 50 mM.

All solutions were prepared with a deionized water of specific resistivity 18.2 MΩ cm (Elix purification system, Millipore). 3 mM NaCl (Merk) were added to the used water to have a defined ionic strength. All experiments were carried out at a room temperature of 25 ± 1 °C.

2.2. Surface tension and surface dilatational rheology

We formed and observed buoyant bubbles on the tip of a J-shaped hollow needle dipped in the aqueous solution by means of the instrument DSA100R (Krüss GmbH, Germany). The surface tension σ was determined by axisymmetric drop shape analysis with the software DSA1 (Krüss GmbH). The surface dilatational storage and loss moduli, E' and E'', were determined using the OBM [34]. For this goal, the variation of σ was recorded for sinusoidal oscillations of the bubble area A with a period of 2 s.

A sketch of the experimental setup [32] for exchange of the aqueous phase is shown in Fig. 1a. A cartridge pump simultaneously supplies the new solution and sucks out the old one with the same flow rate thus keeping the volume of liquid in the cuvette constant. The estimates [31] show that when the volume of the inserted new solution reaches 10 times the volume of the cuvette, the resulting solution becomes practically identical with the newly supplied one. In our experiments, the pump was stopped when the volume of the supplied new solution became 12 times the cuvette volume. The bubble was observed in transmitted light during the whole experiment and its profile was processed to calculate the surface tension, bubble area, volume, and the error of the Laplace fit.

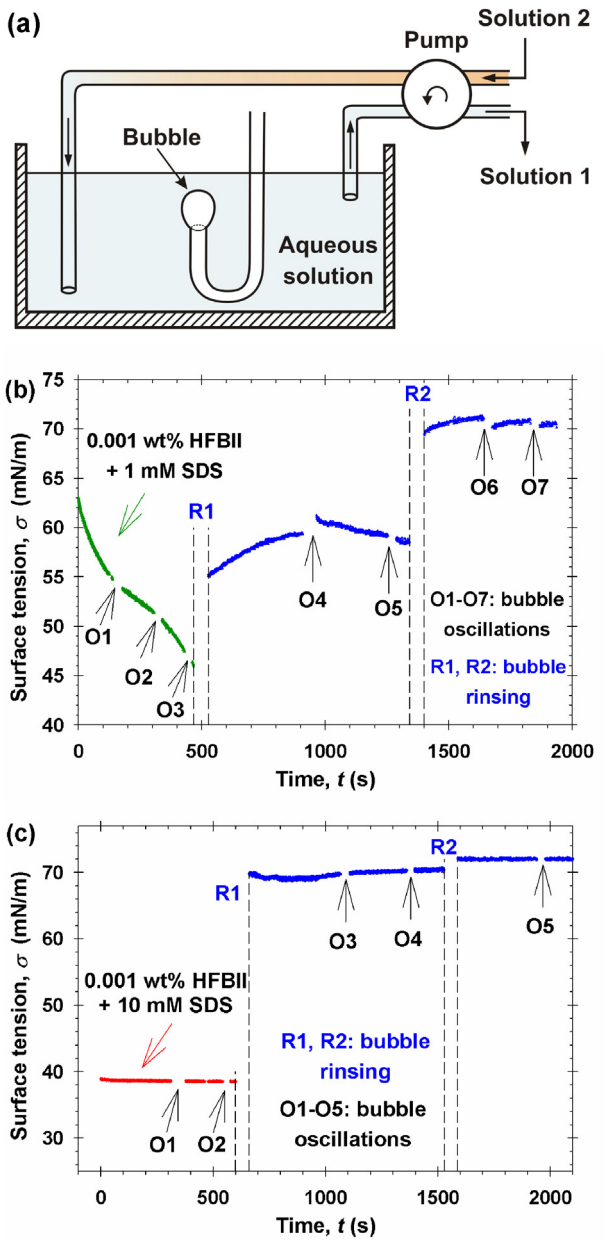

Fig. 1. (a) Setup for exchanging the aqueous phase around a bubble attached to the tip of a capillary. (b) Parallel adsorption from a HFBII + SDS solution at an SDS concentration *below* the CMC. (c) Analogous experiment, but at an SDS concentration *above* the CMC. Phase exchanges (rinsing) with water and oscillation experiments have been applied as denoted in the figure.

The experimental protocol for *parallel* adsorption is as follows. A bubble is formed in a given solution containing surfactant and/or protein. The relaxation of surface tension σ is measured. At different moments during this process, the bubble volume is subjected to oscillations at 0.5 Hz for 30 s to measure the surface dilatational moduli E' and E''; see, e.g., the stages O1, O2 and O3 in Fig. 1b. Next, the solution is exchanged with water (rinsing of the bubble); see the stages R1 and R2 in Fig. 1b and c. The aim of this experiment is to see whether the rinsing can remove HFBII and/or SDS from the bubble surface. This is established by applying bubble oscillations (e.g., O4–O7 in Fig. 1b) to measure again the moduli E' and E''.

In the case of *sequential adsorption* the bubble is formed in the protein solution. After a certain period of time, the solution is exchanged with water. In the case of HFBII (without SDS), this exchange was carried out at a $\sigma > 50$ mN/m, because at $\sigma \leq 50$ mN/m

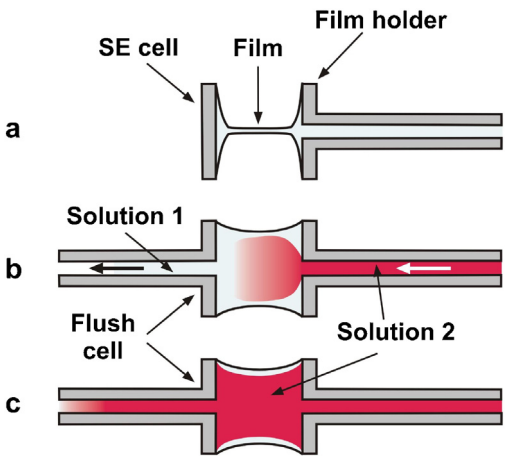

Fig. 2. (a) Scheludko–Exerowa cell [35] for the formation of thin liquid films in the center of a capillary by sucking of liquid through the side tube. (b) The protein solution in the flush cell [36], can be replaced with surfactant solution. (c) Thus, films sandwiched between mixed protein/surfactant layers obtained by sequential adsorption can be studied.

the hydrophobin adsorption layers solidify [3]. Then, as already mentioned, the bubble profile could become non-Laplacian and the automatic bubble-shape analysis would become inapplicable. (For BLG and BSA there is no surface solidification, at least within 2 h.) After the rinsing with water, oscillations have been applied to measure E' and E''. Next, the water is replaced by an SDS solution at a given concentration, and E' and E'' are measured again. This step was repeated several times with increasing SDS concentrations, up to 50 mM, to check whether SDS could wash up the protein adsorbed on the bubble. In some experiments, after the "washing" with SDS, rinsing with water was applied. Experimental curves with sequential adsorption of SDS are shown in Appendix A.

In the experiments on sequential adsorption, the protein (HFBII, BLG or BSA) was always first supplied to the bubble surface. The reason is that the adsorption of the studied proteins is irreversible, at least in the time-scale of our experiments. In contrast, if the surfactant (SDS) is first supplied, it is immediately washed out from the interface during the next phase exchange.

2.3. Thin foam films

Experiments with individual foam films were carried out with the Scheludko–Exerowa (SE) cell [35] (Fig. 2a) and with the flush cell [36] (Fig. 2b and c). In the SE cell, the investigated solution is loaded in a cylindrical capillary through an orifice in its wall. Next, liquid is sucked from the formed biconcave drop until a film appears in the central part of the cell. By injecting or sucking of liquid through the side capillary, one can vary the radius of the formed film. Its thickness can be measured by means of an interferometric method [35]. For this purpose, the light reflected from the film is supplied to a photomultiplier and computer, and the film thickness is recorded in the course of the experiment. The SE cell was used to investigate thin liquid films in the case of *parallel* adsorption of HFBII and SDS on the film surfaces.

In the experiments with the flush cell [36], the protein solution is first supplied in the cell. The protein irreversibly adsorbs on the two surfaces of the biconcave drop. Next, by using the two side capillaries, the protein solution in the cell is replaced with an SDS solution (Fig. 2b and c) and, finally, a liquid film is formed in the middle of the cell. The flush cell was used to investigate thin liquid films in the case of *sequential* adsorption of HFBII and SDS.

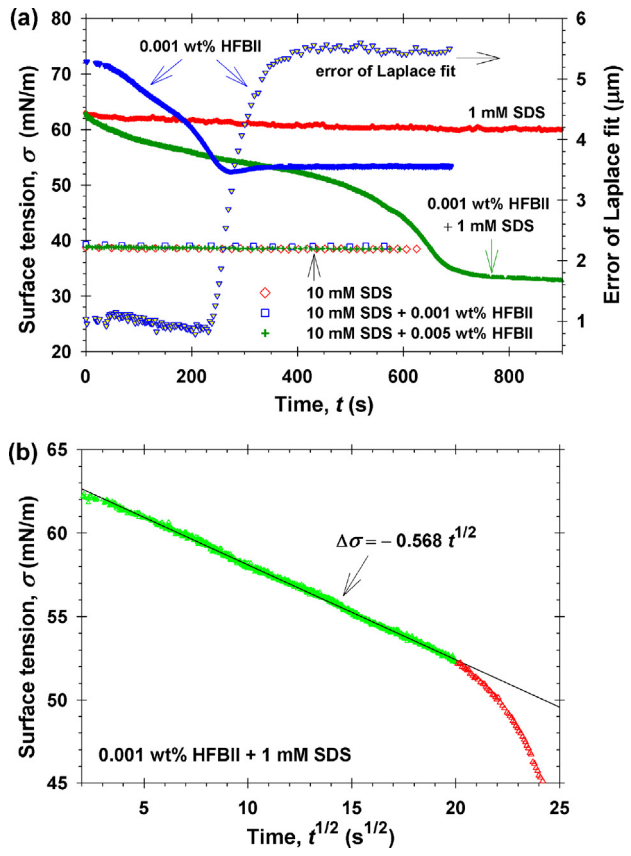

Fig. 3. (a) Surface tension relaxation for solutions of 0.001 wt% HFBII, 1 mM SDS, their mixed solution and for solutions containing 10 mM SDS + 0, 0.001 and 0.005 wt% HFBII. For the first solution, the adsorption layer solidifies, as indicated by rise in the error of the Laplace fit of the bubble profile. (b) Plot of σ vs $t^{1/2}$ indicating diffusion controlled adsorption from a mixed HFBII/SDS solution.

3. Kinetics of parallel adsorption of HFBII and SDS

3.1. Experimental results and discussion

Fig. 3a shows the relaxation of surface tension, σ, with time, t, for buoyant bubbles; σ is determined as an adjustable parameter by fitting the bubble profile with the Laplace equation of capillarity (DSA method). For HFBII solutions, the error of the Laplace fit (shown in Fig. 3a) steeply increases when the decreasing σ reaches ≈53 mN/m. This indicates solidification of the adsorption layer on the bubble surface [3]. Solidification is not observed if SDS is added to the hydrophobin solution at the studied concentrations ≥1 mM.

In the case of solidified adsorption layer, the deviations from the Laplace shape are due to the fact that the surface tension becomes non-uniform (σ depends on the position at the interface) and non-isotropic – the values of σ measured in two perpendicular directions are different, i.e., σ becomes a tensor [37]. Hereafter, all data for σ are obtained with isotropic adsorption layers, for which the error of the Laplace fit is small, so that the DSA method is applicable and yields the correct value of σ.

The surface tension of a solution of 1 mM SDS (below the CMC) relaxes very fast, and for this reason the respective σ-vs-t curve in Fig. 3a is almost horizontal. At $t = 0$, the surface tension of the mixed solution of 0.001 wt% HFBII and 1 mM SDS coincides with that for 1 mM SDS alone. At $t > 0$ the surface tension gradually decreases until reaching an equilibrium value of 33 mN/m after 800 s. Because $\sigma \approx 60$ mN/m for 1 mM SDS alone, the lowering of σ to 33 mN/m can be explained with the relatively slow adsorption of HFBII and the formation of a mixed adsorption layer with the adsorbed SDS. The lower surface tension of the mixed solution (33 vs 60 mN/m) indicates a synergistic interaction of HFBII and SDS at the interface. The large linear portion of the plot of σ vs $t^{1/2}$ in Fig. 3b, can be interpreted as HFBII adsorption under diffusion control; see Section 3.2 for quantitative interpretation.

At 10 mM SDS + 0, 0.001 and 0.005 wt% HFBII the adsorption kinetics is completely different – see the horizontal line corresponding to $\sigma \approx 38.6$ mN/m in Fig. 3a. (10 mM SDS is above the CMC, which is 6.7 mM in the presence of 3 mM NaCl.) In this case, the hydrophobin in the solution produces no effect on its surface tension. Hence, in this case the hydrophobin forms mixed aggregates with SDS in the bulk without adsorbing at the air/water interface. This result is in agreement with the findings by Zhang et al. [18] and holds for the considered case of *parallel* adsorption of SDS and HFBII.

At a given moment during the surface tension relaxation, oscillations of the bubble volume (and surface area) were applied, and the corresponding variations in σ were registered. Analysis of the obtained data yields the surface dilatational storage and loss moduli, E' and E''. Results are shown in Table 1, where each run is characterized by the values of the surface tension σ and surface pressure $\pi_s = 72 - \sigma$ (mN/m) just before the oscillations.

Run 1 in Table 1 corresponds to oscillations of period 2 s around the equilibrium surface tension $\sigma = 60$ mN/m for a solution of 1 mM SDS. The obtained values $E' = 2.7$ and $E'' = 1.2$ (mN/m) are relatively low and typical for conventional water-soluble surfactants. Run 2 in Table 1 corresponds to the initial stage of relaxation of the surface tension of a 0.001 wt% HFBII solution, as indicated by the high surface tension, $\sigma = 70$ mN/m. The measured high storage modulus, $E' = 143.2$ mN/m, indicates the presence of a considerable amount of HFBII at the interface, even at such high σ.

Runs 3 and 4 in Table 1 correspond to two consecutive stages of the relaxation of surface tension of a solution containing 0.001 wt% HFBII + 1 mM SDS. As already discussed in relation to the respective curve in Fig. 3a, the decrease of σ from 51 to 35 mN/m, which is accompanied with a rise of E' from 35.7 to 155.6 mN/m, evidences for the increase of the adsorbed amount of HFBII with time. This result confirms that at concentrations below the CMC of SDS, the hydrophobin molecules can adsorb at the interface, partially displacing the already adsorbed surfactant molecules. The kinetics of this process is considered quantitatively in the next section.

3.2. Kinetics of protein adsorption from a mixed solution with surfactant

As mentioned above, the adsorption of SDS occurs very fast, so that the whole further decrease of σ is due to the slower adsorption of the protein. The linear part of the plot of σ vs $t^{1/2}$ in Fig. 3b can be described as a diffusion-controlled adsorption at the early times. In this case, the equation of Ward and Tordai yields the following asymptotic dependence [38,39]:

$$\Delta\sigma = -2kTc\left(\frac{D}{\pi}t\right)^{1/2} \quad (1)$$

where $\Delta\sigma$ is the variation of surface tension; k is the Boltzmann constant; T is the absolute temperature; c and D are the concentration and diffusivity of the adsorbing species, in our case–the protein. Substituting the experimental values $T = 298$ K, $c = 1.39$ μM and $D = 1.44 \times 10^{-10}$ m^2/s for HFBII (see Appendix A), from Eq. (1) we obtain that the slope of the $\Delta\sigma$-vs-$t^{1/2}$ plot should be −0.0467 mN/(m s$^{1/2}$) which is 12.2 times smaller than the experimental slope in Fig. 3b. The reason for this considerable difference cannot be the bulk aggregation of HFBII, because it would lead to smaller values of c and D, and then the slope calculated from Eq. (1) would become even smaller.

Table 1
Surface moduli E' and E'' measured by the OBM (2 s period), at different surface tension σ and surface pressure π_s.

Run no.	System/stage	σ (mN/m)	π_s (mN/m)	E' (mN/m)	E'' (mN/m)
A. Surface tension relaxation (Fig. 3a)					
1	1 mM SDS[a]	60	22	2.7	1.2
2	0.001 wt% HFBII	70	2	143.2	5.0
3	0.001 wt% HFBII + 1 mM	51	21	35.7	5.0
4	SDS[a]	35	38	155.6	0
B. Parallel adsorption: 0.001 wt% HFBII + 1 mM SDS[a] (Fig. 1b)					
5	After 1st PhE with water[a]	61	11	230	−11
6	After 2nd PhE with water[a]	70	2	149	7.2
C. Parallel adsorption: 0.001 wt% HFBII + 10 mM SDS[a] (Fig. 1c)					
7	The initial solution	38	34	0	0.4
8	After 1st PhE with water[a]	70	2	6.5	1.4
9	After 2nd PhE with water[a]	72	0	0	0
D. Sequential adsorption: the protein is first adsorbed (Figs. A5–A7, Appendix A)					
10	0.001 wt% HFBII	70	2	139.0	5.70
11	After PhE with 10 mM SDS	34	38	30.8	3.62
12	After PhE with water[a]	63	9	227.8	3.3
13	0.01 wt% BLG	53.7	18.5	85.1	12.7
14	After PhE with 10 mM SDS	37.0	35.2	0.8	0.3
15	After PhE with water[a]	70	2.2	0	0
16	0.01 wt% BSA	57.1	15.1	76.8	13.1
17	After PhE with 10 mM SDS	35.1	37.1	8.6	1.9
18	After PhE with water[a]	71.5	0.7	0	0

[a] The water contains 3 mM NaCl; PhE denotes "phase exchange".

This discrepancy can be overcome if the presence of SDS (together with the HFBII) at the interface is taken into account. A model that is applicable to mixed adsorption of proteins and surfactants was recently developed and applied to various systems by Fainerman, Miller et al. [40–44]. This model takes into account different possible conformational states of the protein molecules at the interface. Because HFBII is a rigid molecule that is not expected to undergo conformational changes upon adsorption, here it is convenient to apply the simpler van der Waals adsorption model [45,46], generalized for a two-component solution [47], viz. HFBII + SDS. An advantage of the latter model is that the parameters α_{ij} that account for the area exclusion effect (see below) can be directly estimated from the molecular cross-sectional areas, which are in principle known; see e.g. Table 4 in Ref. [48]. The van der Waals model leads to the following generalized form of Eq. (1) (see Appendix A):

$$\Delta\sigma = -2kTcB\left(\frac{D}{\pi}t\right)^{1/2} \tag{2}$$

where the dimensionless coefficient B is defined as follows:

$$B = B_{hc} - B_{int}, \quad B_{hc} = \frac{1 + 2(\alpha_{14} - \alpha_{11})\Gamma_1}{(1 - \alpha_{11}\Gamma_1)^2}, \quad B_{int} = 2\frac{\beta_{14}\Gamma_1}{kT} \tag{3}$$

Here, the same numbering of the components as in Ref. [47] is used, viz. 1 stands for the dodecylsulfate anion and 4 for the protein (HFBII); Γ_1 is the adsorption of SDS in the absence of HFBII; α_{11} and α_{14} are excluded surface areas; the parameter β_{14} accounts for the interaction between the SDS and HFBII molecules; positive β_{14} (and B_{int}) would mean that the attractive interactions prevail [47]. B_{hc} accounts for the effect of the hard core (excluded area) interactions, whereas B_{int} accounts for the effect of all other interactions, including the van der Waals and hydrophobic forces between the HFBII and SDS molecules. Using the model in Ref. [47], we calculated that $\alpha_{11}\Gamma_1 = 0.372$ for the surface of a solution of 1 mM SDS in the presence of 3 mM NaCl. By molecular size considerations (from the cross-sectional areas of the respective molecules), we determine $\alpha_{11} = 0.30\,nm^2$ and $\alpha_{14} = 2.39\,nm^2$ (see Appendix A). With these parameter values, from Eq. (3) we calculate $B_{hc} = 15.6$, which is close (but slightly greater) than the experimental value $B = 12.2$, determined from the slope of the line in Fig. 3b. The difference $B_{int} = 15.6 - 12.2 = 3.4$ can be interpreted as a contribution of the interactions between the SDS and HFBII molecules. This value of B_{int} corresponds to $\beta_{14}/\beta_{11} = 3.39$, where β_{11} is the respective interaction parameter for two SDS molecules [47]: $2\beta_{11}/(kT\alpha_{11}) = 2.73$. In other words, the energy of interaction between the molecules of SDS and HFBII turns out to be 3.39 times greater than the interaction energy between two adsorbed SDS molecules, which can be due to the van der Waals interaction between their hydrocarbon tails across air.

The obtained numerical results seem reasonable and give an interpretation of the 12.2 times greater slope of the experimental time-dependence in comparison with that predicted by Eq. (1). The effect is explained with the interaction of the adsorbing HFBII molecules with the SDS molecules at the interface. This interaction is dominated by the hard-core (excluded area) effect insofar as $B_{hc} = 15.6$ is considerably greater than $B_{int} = 3.4$ (see above). Note that the early-time asymptotics, $\sigma \propto t^{1/2}$ in Fig. 3b, spans over $\Delta\sigma \approx 20$ mN/m, which is considerably greater than for a single protein. The difference is due to the presence of pre-adsorbed surfactant – the above estimates indicate that its effect is large enough to provide the experimental value of B.

4. Parallel adsorption with phase exchanges

4.1. Experiments with oscillating bubbles

As in Section 3, here we consider parallel adsorption of SDS and HFBII. Here, the difference is that after a certain period of relaxation, the aqueous solution of HFBII + SDS is replaced with water. This "rinsing" of the bubble with water was applied to investigate whether the water could wash out the adsorbed molecules from the interface.

Run 5 in Table 1 corresponds to the oscillatory experiment O4 in Fig. 1b, which was carried out after the adsorption from a solution of 0.001 wt% HFBII + 1 mM SDS (below the CMC), followed by rinsing with water. The rise of σ from 46 mN/m (before the rinsing) to 61 mN/m (after the rinsing) evidences for the washing out of SDS from the adsorption layer. The high storage modulus, $E' = 230$ mN/m measured after the first rinsing, indicates that the HFBII has not been washed out from the bubble surface. The

negative E'' determined in Run 5 is an artifact due to the scattering of the experimental points of the oscillatory dependence $\sigma(t)$. In all experiments, in which HFBII is present at the interface, the Lissajous plots of stress vs. strain indicate purely elastic behavior (see Section 6). In such cases, non-zero values of the loss modulus E'' appear because of the inevitable scattering of the experimental data, but these values do not reflect any measurable effect of surface viscosity. (In contrast, the values of E'' determined for BLG adsorption layers reflect a true surface dilatational viscosity; see below.)

Run 6 in Table 1 corresponds to average values from the oscillatory experiments O6 and O7 in Fig. 1b, which have been carried out after the second phase exchange (rinsing) with water. The rise of σ from 61 to 70 mN/m (at constant bubble surface area) indicates that the first rinsing has been insufficient to completely remove the SDS from the mixed adsorption layer with HFBII. The values of σ and E' after the second rinsing (Run 6) are very close to those for HFBII alone (Run 2), so that one can conclude that SDS has been completely washed out after the second rinsing, i.e. the attachment of SDS molecules to the hydrophobin is reversible.

Run 8 in Table 1 corresponds to the oscillatory experiments O3 and O4 in Fig. 1c, which have been carried out after the adsorption from a solution of 0.001 wt% HFBII + 10 mM SDS (above the CMC), followed by rinsing with water. The rise of σ from 38 mN/m (before the rinsing) to 70 mN/m (after the rinsing) evidences for the washing out of SDS from the adsorption layer. Hydrophobin was not present at the interface before the rinsing, as indicated by the value $E' = 0$ of the storage modulus (Run 7 in Table 1 corresponding to O1 and O2 in Fig. 1c). The value $E' = 6.5$ mN/m measured after the first rinsing (Run 8) can be attributed to the adsorption of a small amount of HFBII molecules (from the disassembling bulk aggregates with SDS) during the first rinsing. After the second rinsing we obtained $\sigma = 72$ mN/m and $E' = 0$ (Run 9 in Table 1 and experiment O5 in Fig. 1c), which means that both the surfactant and the protein have been completely washed out.

4.2. Experiments with thin liquid films

The experimental results for the way of film thinning, the film lifetime, the thickness of the equilibrium film, and the presence of trapped aggregates bring information about the structure of the adsorption layers; about the surface forces acting in the film and its stability. Fig. 4a represents a photograph of the stable equilibrium film of uniform thickness $h = 20$ nm formed in a SE cell (Fig. 2a) from a solution of 0.001 wt% HFBII + 10 mM SDS (above the CMC of SDS). This is a typical foam film stabilized by SDS. No indications for the presence of HFBII (e.g. slower film thinning and HFBII aggregates [14,15]) are seen.

Fig. 4b is obtained with the flush cell (Fig. 2b and c). First, the solution of HFBII + SDS (of the same composition as that for Fig. 4a) is loaded in the cell and adsorption layers are formed at the film surfaces. After 10 min, the liquid in the cell was exchanged with water, and a film was formed. This film was unstable – it ruptured 1 min after its formation. This result indicates the absence of both surfactant and protein at the film surfaces.

The experiments in Fig. 4a and b (parallel adsorption) confirm that if the concentration of SDS is *above* the CMC, the whole amount of HFBII is in the bulk of solution (supposedly, in the form of joint aggregates with SDS); adsorption of HFBII at the air/water interface is not detected.

Fig. 4c and d are photographs of two consecutive stages of the evolution of a foam film formed in a SE cell from a solution of 0.001 wt% HFBII + 1 mM SDS, *below* the CMC of SDS. The interference pattern indicates that initially the film has a lens-shaped cross-section, thicker in the middle and thinner at the periphery, where the formation and expansion of a uniformly thin black film begins

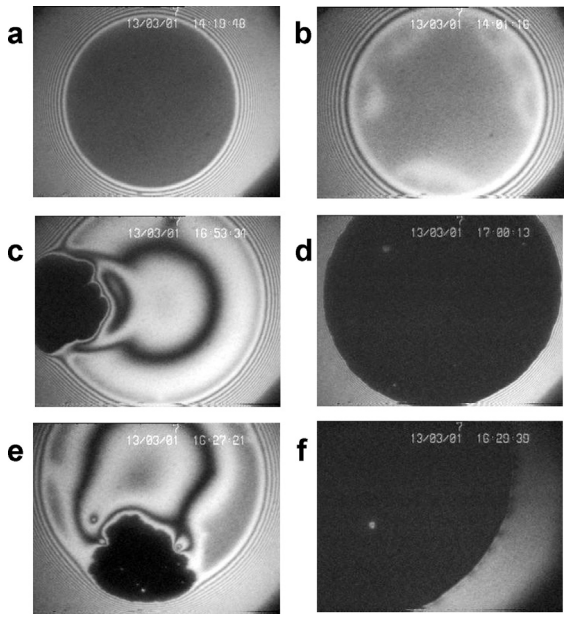

Fig. 4. (a) Stable foam film of thickness $h = 20$ nm from a solution of 0.001 wt% HFBII + 10 mM SDS (SE cell). (b) Unstable film of age 1 min (just before its rupture) formed from the same solution, with a subsequent flushing with water (flush cell). (c) and (d) Two stages of the formation of a stable black film, $h = 11.4$ nm, from a solution of 0.001 HFBII + 1 mM SDS (SE cell). (e) and (f) Two stages of the appearance of a stable black film, $h = 11.1$ nm, formed from the same solution, with a subsequent flushing with water (flush cell).

(Fig. 4c). This stable black film of thickness $h = 11.4$ nm expands until completely displacing the thicker film of non-uniform thickness.

Fig. 4e and f are analogous to Fig. 4c and d, but this time the film is formed in the flush cell. The cell was first loaded with the solution of 0.001 wt% HFBII + 1 mM SDS. After 10 min, the liquid in the cell was exchanged with water, and a film was formed in the middle of the cell. Black film appears again and its thickness is 11.1 nm (Fig. 4e and f). In other words, the film evolution is similar irrespective of whether the protein + surfactant solution has been exchanged with water. Such behavior indicates the presence of irreversibly adsorbed hydrophobin molecules that decelerate the thinning of the film and enhance its stability.

The relatively small thickness of the black films in Fig. 4d and f, $h \approx 11$ nm, as compared with $h = 20$ nm for the electrostatically stabilized film with SDS (Fig. 4a), indicates that in the presence of HFBII the surface concentration of SDS is not so high. (Otherwise, the anionic SDS would lead to a strong electrostatic repulsion between the film surfaces and to the formation of a thicker film.) These black films are probably stabilized by sandwiched small HFBII aggregates, e.g. tetramers [14,15]. In the presence of SDS, the amount of large (visible by microscope) HFBII aggregates in the films is markedly smaller than in the absence of SDS. Probably, the enhanced electrostatic repulsion due to the binding of DS^- anions to the HFBII molecules suppresses the formation of large protein aggregates.

The experiments illustrated in Fig. 4c–f (parallel adsorption) confirm that if the SDS concentration is *below* the CMC, the SDS cannot prevent the adsorption of HFBII at the air/water interface.

5. Sequential adsorption with phase exchanges

5.1. Experiments with buoyant bubbles in HFBII solutions

In this series of experiments, the bubble is first formed in a HFBII solution. Soon after that, the aqueous phase is exchanged with water. Next, the water phase is replaced with an SDS solution.

This phase exchange can be repeated several times at increasing SDS concentrations. For example, in the experiment illustrated in Fig. A5 (Appendix A) the water phase was exchanged consecutively with solutions of 1, 10, 20 and 50 mM SDS. Finally, the aqueous phase was replaced with water, and E' was measured in oscillation experiments to verify whether any HFBII has remained at the interface after this abundant rinsing of the bubble with SDS solutions. Oscillatory experiments have been performed also at intermediate stages of this procedure.

Illustrative results are shown in Table 1, Runs 10, 11 and 12, corresponding to the oscillatory experiments O1, O5 and O12 in Fig. A5 (Appendix A). The comparison of Runs 10 and 11 shows that the exchange of the 0.001 wt% HFBII solution with 10 mM SDS solution leads to a decrease of σ from 70 to 34 mN/m and to a drop of E' from 139 to 30.8 mN/m. At the higher concentrations of SDS (20 and 50 mM), the values of σ and E' are close to those with 10 mM SDS. Finally, after a double rinsing with water, we measured $\sigma = 63$ mN/m and $E' = 230$ mN/m (Run 12 in Table 1). The high value of E' indicates that the HFBII has not been displaced from the interface after rinsing with micellar SDS solutions of concentrations up to 50 mM. Similar are the results from the experiments on sequential adsorption of HFBII and SDS illustrated in Figs. A3 and A4 in Appendix A.

Having in mind that the adsorbed HFBII has not been displaced by the SDS, the considerable decrease of E' from 139 to 30.8 mN/m upon the addition of SDS (Runs 10 and 11) means that the intercalation of SDS molecules between the adsorbed HFBII molecules markedly reduces the elasticity of the adsorption layer.

5.2. Experiments with bubbles in solutions of BLG and BSA

Using the same experimental procedure, we performed sequential adsorption experiments also with the globular proteins BLG and BSA in order to compare the results with those for hydrophobin. Because BLG and BSA are of higher molecular weight and lower surface activity than HFBII, they were used at a 10 times higher concentration, viz. 0.01 wt%. In accordance with Refs. [19–21], displacement of BLG and BSA by SDS is expected.

The obtained values of the surface tension and surface dilatational moduli are given in Table 1 (see Runs 13, 14 and 15 for BLG and Runs 16, 17 and 18 for BSA). In agreement with literature data, our results indicate that SDS displaces the adsorbed BSA and BLG from the air/water interface [19,30,31]. For 0.01 wt% BLG, we measured surface storage modulus $E' = 85$ mN/m at surface pressure $\pi_s = 18.5$ mN/m (Run 13), which coincided with the value measured in Ref. [49] (see Fig. 3 therein).

The exchange of the BLG solution with SDS solution (Run 14) leads to a decrease of σ from 53.7 to 37.0 mN/m, and E' from 85 to 0.8 mN/m. Finally, the rinsing with water (Run 15 in Table 1) yields the values $\sigma = 70$ mN/m and $E' = 0$, which are close to the respective values for the surface of pure water.

For 0.01 wt% BSA, we measured surface storage modulus $E' = 76.8$ mN/m at surface pressure $\pi_s = 15.1$ mN/m (Run 16), which also coincides with the respective value in Ref. [49] (see Fig. 4 therein). The exchange of the BSA solution with SDS solution (Run 17) decreased σ from 57.1 to 35.1 mN/m, and E' from 76.8 to 8.6 mN/m. Finally, the rinsing with water (Run 18 in Table 1) yields the values $\sigma = 71.5$ mN/m and $E' = 0$, i.e. SDS has completely washed out the BSA from the interface.

Our experimental results confirm again that the HFBII adsorption layers have much higher dilatational elasticity than those of other globular proteins [3]. Furthermore, they reveal another exceptional property of the HFBII molecules – having once adsorbed on the air/water interface they cannot be displaced by an anionic surfactant, like SDS.

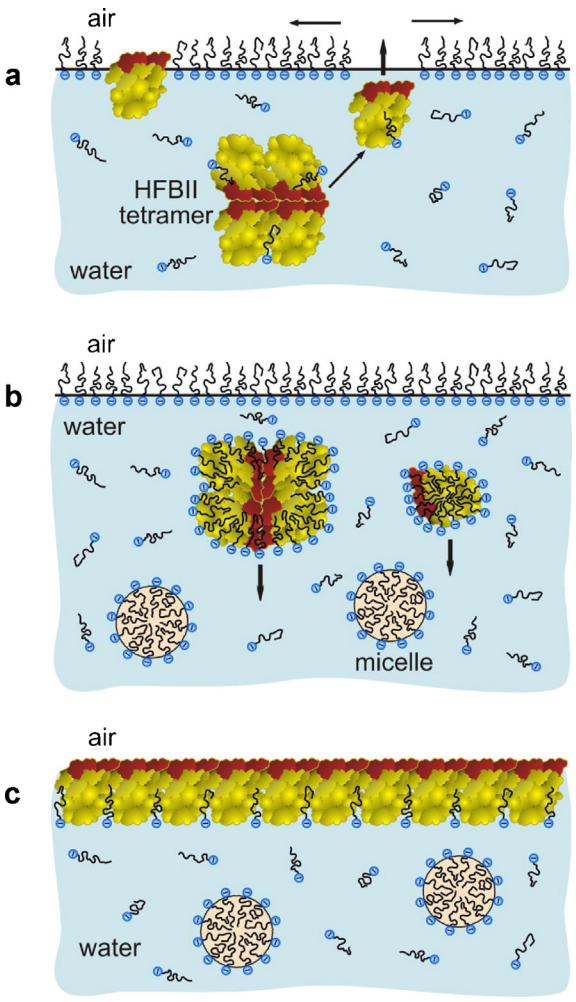

Fig. 5. (a) In the case *parallel* adsorption from HFBII + SDS solutions *below* the CMC, the HFBII adsorbs slower than SDS and mixed adsorption layers are formed. (b) In the case of *parallel* adsorption *above* the CMC, the HFBII forms mixed aggregates with SDS in the bulk and does not adsorb at the air/water interface. (c) In the case of *sequential* adsorption, having first adsorbed at the interface, the HFBII cannot be displaced by SDS, even at concentrations above the CMC.

5.3. Parallel vs sequential adsorption – discussion

In summary, our experiments on *parallel* adsorption indicate that if the SDS concentration is *below* the CMC, the HFBII adsorbs at the air/water interface, partially displacing the faster adsorbing SDS (Fig. 5a). In contrast, at SDS concentrations *above* the CMC the hydrophobin molecules and aggregates in the bulk are hydrophilized by the SDS (Fig. 5b). Thus, if HFBII is dissolved in a micellar SDS solution, the HFBII molecules form joint aggregates with the SDS, whereas the air/water interface remains free of HFBII molecules.

The experiments on *sequential* adsorption demonstrated that having once adsorbed at the air/water interface the HFBII cannot be displaced from there if the protein solution is exchanged with a micellar solution of SDS (Fig. 5c). In contrast, if the same experiment is executed with BLG or BSA (instead of HFBII), the results show that BLG and BSA are completely washed out from the interface by micellar SDS solutions. As already mentioned, an additional unique property of hydrophobin in comparison with the other proteins is that the adsorption energy of HFBII is so high that it cannot be displaced from the air/water interface by an ionic surfactant as SDS. However, the SDS can displace other adsorbed proteins, such

as BLG, BSA and β-casein. The mechanism of such displacement was revealed by Mackie et al. [19–21].

The obtained results indicate also the existence of *two metastable states* for the HFBII molecules in contact with a micellar SDS solution: (i) aggregates of HFBII + SDS in the bulk (Fig. 5b) and (ii) adsorption layer at the air/water interface (Fig. 5c). The fact that depending on the experimental procedure (parallel or sequential adsorption) we obtain either the first or the second state means that these two states are separated by a sufficiently high energy barrier. From this viewpoint, the joint aggregates of HFBII and SDS differ from the conventional surfactant micelles, which readily exchange molecules with the solution's surface.

6. Dilatational elasticity vs surface tension

In the previous sections, the dilatational elasticity was characterized with the storage modulus E'. Because E' was used as an indicator for the presence of adsorbed protein, special values of E' were sufficient for our purpose; see Table 1. However, the systematization of the accumulated experimental data with oscillating bubbles would allow us to extract additional information, viz. to determine the dependence of the surface dilatational elasticity on the surface tension σ.

6.1. Lissajous plots and cumulative curve

In the oscillatory experiments, the bubble surface area $A(t)$, and the surface tension $\sigma(t)$ oscillate with a period of $2\pi/\omega$ around the mean values of these parameters, A_m and σ_m; ω is the angular frequency. As a rule, the relative changes in the surface area are small, $A(t) - A_m \ll A_m$, so that the surface dilatation, $\alpha(t)$, can be expressed in the form:

$$\alpha(t) \equiv \ln\left[\frac{A(t)}{A_m}\right] \approx \frac{A(t) - A_m}{A_m} = \alpha_a \sin(\omega t) \tag{4}$$

where α_a is the dilatation amplitude. For small amplitudes, $\sigma(t)$ oscillates with the same period as $\alpha(t)$, and can be expressed in the form:

$$\frac{\sigma(t) - \sigma_m}{\alpha_a} = E' \sin(\omega t) + E'' \cos(\omega t) \tag{5}$$

Knowing α_a, one determines E' and E'' from the fit of the experimental $\sigma(t)$ dependence with Eq. (5).

The Lissajous curve represents the plot of the stress, $\sigma(t) - \sigma_m$, vs strain, $\alpha(t)$ [5]. If Eqs. (4) and (5) are satisfied, the Lissajous curve represents an ellipse. This is illustrated in Fig. 6a with data for the oscillatory experiment corresponding to Run 13 with 0.01 wt% BLG in Table 1. In view of Eq. (5), the semi-minor axis of the ellipse in Fig. 6a is proportional to the loss modulus E''. Because the scattering of the experimental points in this figure is much smaller than the length of the semi-minor axis, we can conclude that E'' is accurately determined in this experiment.

For HFBII adsorption layers, the situation is different. Fig. 6b shows data from oscillatory experiments from Figs. A4 and A5 in Appendix A (the upper and lower branches, respectively). Each segment in Fig. 6b, which is the Lissajous plot for an oscillatory experiment, represents a segment – a degenerated ellipse at $E'' \to 0$. The minor semi-axis of this degenerated ellipse is comparable with the scattering of the experimental points. Hence, E'' is zero in the frames of the experimental accuracy for each of these runs. In such a case, the most reliable value of elasticity can be determined from the slope of the respective segment in Fig. 6b. The surface dilatational elasticity, E_{dil}, determined in this way is [50]:

$$E_{dil} = -\frac{d\sigma}{d\ln(A/A_0)} \tag{6}$$

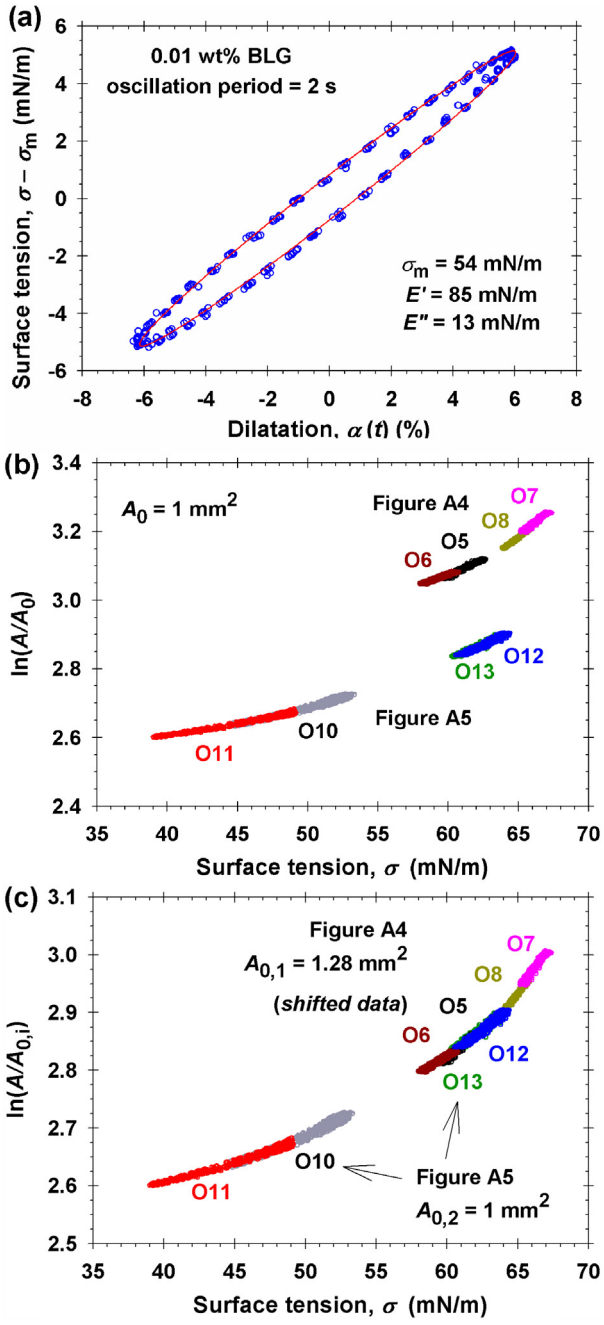

Fig. 6. (a) Lissajous plot of the stress, $\sigma - \sigma_m$, vs dilatation, $\alpha(t)$ for the adsorption layer from 0.01 wt% BLG solution (Run 13 in Table 1). (b) Plots of $\ln(A/A_0)$ for oscillating bubbles with HFBII/SDS adsorption layers after rinsing with water–data from Figs. A4 and A5 in Appendix A. (c) The same plots, but the data from Fig. A4 are shifted downwards (rescaled with $A_{0,1}$) to lie on the curve with data from Fig. A5.

As before, $A = A(t)$ is the interfacial area, whereas A_0 is a constant reference area that scales A. For example, $A_0 = 1\,mm^2$ in Fig. 6b expresses the measurement units of A. As seen from Eq. (6), the value of E_{dil} is independent of the choice of A_0.

In our experiments (like those in Fig. 6b) the adsorption of HFBII was initially ceased by exchanging the hydrophobin solution with water (to avoid surface solidification; see above). In different experiments, this procedure leads to the adsorption of different amounts of HFBII on bubbles of different surface area. This is the reason for the difference between the two branches of Lissajous curves in Fig. 6b obtained from Figs. A4 and A5 in Appendix A.

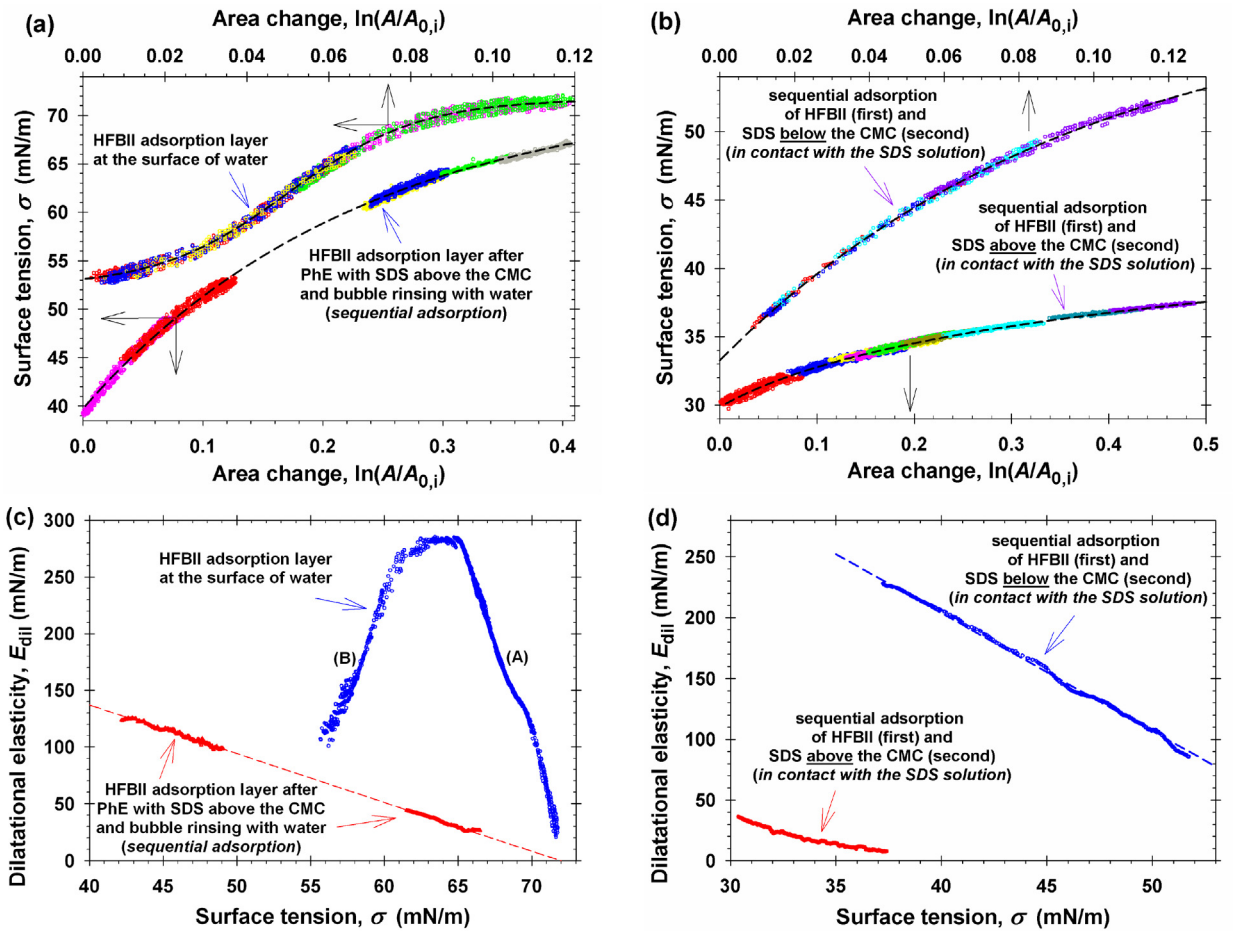

Fig. 7. Cumulative dependencies of σ on $\ln(A/A_{0,i})$ (a) for adsorption layers from HFBII + SDS rinsed with pure water, and (b) for HFBII first adsorbed and then rinsed with an SDS solution. (c) and (d) E_{dil} obtained by differentiation of the σ-vs-$\ln(A/A_{0,i})$ dependencies in (a) and (b), respectively, in accordance with Eq. (6).

The above difference can be overcome in the following way. We can shift the experimental curves originating from Fig. A4 downwards along the vertical axis until they lay on the experimental dependence originating from Fig. A5, as shown in Fig. 6c. Because our goal is to determine E_{dil} from the slope of the experimental curve using Eq. (6), such a shift is permitted because it corresponds to a re-definition of the scaling parameter A_0 for the respective set of data–the value of E_{dil} is independent of the choice of A_0 (see above). The data from Figs. A4 and A5 in Fig. 6c correspond to two different values of the scaling parameter, $A_{0,1}$ and $A_{0,2}$ respectively, which are given in the figure.

In this way, we can select one of the $\ln(A/A_0)$-vs-σ curves (corresponding to a given experiment) as a template and to translate the data from all other experiments (of the same type) on the selected curve, thus, obtaining a cumulative master curve. Next, the cumulative curve can be differentiated numerically, in accordance with Eq. (6), to determine the dependence of E_{dil} on σ. The differentiation can be carried out accurately, using an appropriate numerical method [51]. The collapse of all available data on a single cumulative curve broadens the statistical basis for determining the E_{dil}-vs-σ dependence.

6.2. Results for the surface dilatational elasticity

The upper curve in Fig. 7a represents the cumulative master curve for all oscillatory experiments with HFBII adsorption layers that do not contain SDS. This set of data includes data from oscillatory experiments performed with the initial HFBII layers before the phase exchanges, or after the rinsing of the bubbles with water in the course of experiments on parallel and sequential adsorption at SDS concentration *below* the CMC (1 mM). The lower curve in Fig. 7a is the cumulative curve for similar oscillatory experiments on sequential adsorption, carried out after the exchange of an SDS solution of concentration *above* the CMC with water. For both curves in Fig. 7a, the HFBII film lays on the surface of water, but for the lower curve the layer may contain some amount of SDS insofar as a single rinsing turns out to be insufficient to completely remove the adsorbed SDS if its initial concentration has been above the CMC.

The two curves in Fig. 7c represent E_{dil} calculated by differentiation of the respective cumulative dependencies in Fig. 7a in accordance with Eq. (6). The upper curve exhibits a remarkable non-monotonic behavior with a maximum of height $E_{dil} = 284$ mN/m, close to that determined with pendant drops [3]. Such a maximum in the E_{dil}-vs-σ dependence has been observed for other proteins at the air/water and oil/water interfaces [49,52], but its height is considerably lower than that for HFBII. Analogous maximum has been observed also for triblock copolymers (PEO–PPO–PEO and PPO–PEO–PPO) at the air/water interface [53], which means that the phenomenon is not specific for proteins, but has a more general character. A possible interpretation in terms of surface phase transition is discussed in Section 5 of Appendix A.

The lower curve in Fig. 7c is in fact a straight line of intercept corresponding to $E_{dil} = 0$ at $\sigma = 72$ mN/m (clean water surface). The significant difference between the two E_{dil}-vs-σ dependencies in Fig. 7c can be explained with the effect of SDS: the upper curve

with the maximum represents the dilatational elasticity of an HFBII adsorption layer without SDS, whereas the lower curve represents the elasticity of an HFBII layer containing SDS molecules that have remained after the exchange of the micellar SDS solution with water.

This interpretation is supported by the data in Fig. 7b and d. The data in Fig. 7b represent cumulative master curves for all oscillatory experiments on sequential adsorption of HFBII and SDS, at which the HFBII adsorption layer is in contact with an SDS solution of concentration below the CMC (the upper curve) and above the CMC (the lower curve). The two curves in Fig. 7d represent E_{dil} calculated by differentiation of the curves in Fig. 7b in accordance with Eq. (6). The upper curve in Fig. 7d is similar to the linear dependence in Fig. 7c. The lower curve corresponds to markedly lower E_{dil} values, which, nevertheless, are significantly higher than those for SDS alone. The additional lowering of E_{dil} can be attributed to the nucleation of spots occupied by SDS within the interfacial protein network when the bulk SDS concentration is above the CMC, as observed elsewhere with similar systems [21]. It is remarkable that the HFBII interfacial network is restored after washing off the SDS – compare the values of E' for Runs 11 and 12 in Table 1.

The linear dependencies in Figs. 7c and d can be described with the empirical equation $E_{dil} = n(\sigma_0 - \sigma)$, where n is the dimensionless slope of the line. Combining the definition of surface elasticity with this linear dependence,

$$\frac{d\sigma}{E_{dil}(\sigma)} = d\ln\Gamma, \qquad E_{dil} = n(\sigma_0 - \sigma) \tag{7}$$

(with Γ being the protein adsorption) and integrating, we obtain the surface equation of state:

$$\sigma = \sigma_0 - kT\Gamma_s\left(\frac{\Gamma}{\Gamma_s}\right)^n \tag{8}$$

Γ_s is an integration constant that may depend on temperature. For the lower line in Fig. 7c we determine $n = 4.30 \pm 0.01$ and $\sigma_0 = 72$ mN/m (the surface tension of air/water interface without SDS), whereas for the upper line in Fig. 7d we find $n = 9.70 \pm 0.03$ and $\sigma_0 = 61$ mN/m (the surface tension of 1 mM SDS solution without HFBII).

As discussed in Section 5 of Appendix A, the right branch (A) of the curve in Fig. 7c could be explained as compression of a two-dimensional gas of adsorbed charged protein molecules and aggregates, whereas the left branch (B) can be due to a phase transition, i.e., merging of aggregates upon a further compression. Finally, the percolation threshold (solidification), i.e. the formation of an elastic network that spans the whole interface, occurs at $\sigma \approx 53$ mN/m, as indicated by the rise of the error of the Laplace fit in Fig. 3a.

7. Summary and conclusions

This study is dedicated to the adsorption kinetics and dilatational surface rheology of interfacial layers from the protein hydrophobin, and its interactions with a surfactant (SDS) at the interface. The dynamic surface tension, as well as the surface storage and loss dilatational moduli, was determined from the profile of buoyant bubbles formed at the tip of a capillary. The oscillating bubble method was used, and experiments with thin foam films were carried out. The most important results are as follows.

The experiments indicate that there is a significant difference between the results from the parallel and sequential adsorption of HFBII and SDS, which is illustrated in Fig. 5. Having first adsorbed at the air/water interface, the HFBII cannot be washed out by a micellar SDS solution, which is not the case with other proteins (BLG, BSA). The results indicate also the existence of *two metastable states* for the HFBII molecules in contact with a micellar SDS solution: (i) aggregates of HFBII + SDS in the bulk (Fig. 5b) and (ii) adsorption layer at the air/water interface (Fig. 5c). The fact that depending on the experimental procedure (parallel or sequential adsorption) we obtain either the first or the second state means that these two states are separated by a sufficiently high energy barrier.

In the case of parallel adsorption of HFBII and SDS, the slope of the experimental surface-tension relaxation curve is about 12 times greater than predicted by the conventional relaxation formula. A quantitative explanation of this effect is given: The greater slope of the relaxation curve is due to the intercalation of slower adsorbing protein molecules between the pre-adsorbed surfactant molecules; see Section 3.2.

A new procedure for data processing is proposed, which allows one to create a single cumulative master curve by collecting data from many different runs with oscillating bubbles (carried out at different surface tensions); see Fig. 6. The differentiation of this curve yields the dependence of the dilatational surface elasticity, E_{dil}, on the surface tension, σ, with a greater reliability because of the broader statistical basis.

Two different types of E_{dil} vs. σ dependences have been found (Fig. 7c and d): straight line and curve with maximum. The former type of dependence could be interpreted with the compression/expansion of a surface "gas" of adsorbed protein molecules and aggregates, whereas the latter one – with a surface phase transition, viz. mergence of smaller aggregates into bigger ones; see Ref. [49] and Fig. A8 in Appendix A. The results could contribute to a deeper understanding of the factors that control the properties of hydrophobin interfacial layers and mixed protein/surfactant layers in relation to the various potential applications of such systems.

Acknowledgments

The authors gratefully acknowledge the support from Unilever Research, Grant No. VL-2011-0699; from the FP7 project Beyond-Everest, and from COST Actions CM1101 and MP1106.

Appendix A. Supplementary data

Supplementary data associated with this article can be found, in the online version, at http://dx.doi.org/10.1016/j.colsurfa.2014.06.002.

References

[1] M.B. Linder, Hydrophobins: proteins that self assemble at interfaces, Curr. Opin. Colloid Interface Sci. 14 (2009) 356–363.
[2] T.B.J. Blijdenstein, P.W.N. de Groot, S.D. Stoyanov, On the link between foam coarsening and surface rheology: why hydrophobins are so different, Soft Matter 6 (2010) 1799–1808.
[3] N.A. Alexandrov, K.G. Marinova, T.D. Gurkov, K.D. Danov, P.A. Kralchevsky, S.D. Stoyanov, T.B.J. Blijdenstein, L.N. Arnaudov, E.G. Pelan, A. Lips, Interfacial layers from the protein HFBII hydrophobin: dynamic surface tension, dilatational elasticity and relaxation times, J. Colloid Interface Sci. 376 (2012) 296–306.
[4] G.M. Radulova, K. Golemanov, K.D. Danov, P.A. Kralchevsky, S.D. Stoyanov, L.N. Arnaudov, T.B.J. Blijdenstein, E.G. Pelan, A. Lips, Surface shear rheology of adsorption layers from the protein HFBII hydrophobin: effect of added β-casein, Langmuir 28 (2012) 4168–4177.
[5] K.D. Danov, G.M. Radulova, P.A. Kralchevsky, K. Golemanov, S.D. Stoyanov, Surface shear rheology of hydrophobin adsorption layers: laws of viscoelastic behavior with applications to long-term foam stability, Faraday Discuss. 158 (2012) 195–221.
[6] E. Aumaitre, S. Wongsuwarn, D. Rossetti, N.D. Hedges, A.R. Cox, D. Vella, P. Cicuta, A viscoelastic regime in dilute hydrophobin monolayers, Soft Matter 8 (2012) 1175–1183.
[7] J. Burke, A. Cox, J. Petkov, B.S. Murray, Interfacial rheology and stability of air bubbles stabilized by mixtures of hydrophobin and β-casein, Food Hydrocolloids 34 (2014) 119–127.
[8] A.R. Cox, D.L. Aldred, A.B. Russell, Exceptional stability of food foams using class II hydrophobin HFBII, Food Hydrocolloids 23 (2009) 366–376.
[9] M. Reger, T. Sekine, T. Okamoto, H. Hoffmann, Unique emulsions based on biotechnically produced hydrophobins, Soft Matter 7 (2011) 8248–8257.

[10] N.D. Denkov, S. Tcholakova, K. Golemanov, A. Lips, Jamming in sheared foams and emulsions, explained by critical instability of the films between neighboring bubbles and drops, Phys, Rev. Lett. 103 (2009) 118302.
[11] M. Qin, L.-K. Wang, X.-Z. Feng, Y.-L. Yang, R. Wang, C. Wang, L. Yu, B. Shao, M.-Q. Qiao, Bioactive surface modification of mica and poly(dimethylsiloxane) with hydrophobins for protein immobilization, Langmuir 23 (2007) 4465–4471.
[12] X. Li, S. Hou, X. Feng, Y. Yu, J. Ma, L. Li, Patterning of neural stem cells on poly(lactic-co-glycolic acid) film modified by hydrophobin, Colloids Surf. B 74 (2009) 370–374.
[13] S. Askolin, M. Linder, K. Scholtmeijer, M. Tenkanen, M. Penttila, M.L. de Vocht, H.A.B. Wosten, Interaction and comparison of a class I hydrophobin from *Schizophyllum commune* and class II hydrophobins from *Trichoderma reesei*, Biomacromolecules 7 (2006) 1295–1301.
[14] E.S. Basheva, P.A. Kralchevsky, N.C. Christov, K.D. Danov, S.D. Stoyanov, T.B.J. Blijdenstein, H.-J. Kim, E.G. Pelan, A. Lips, Unique properties of bubbles and foam films stabilized by HFBII hydrophobin, Langmuir 27 (2011) 2382–2392.
[15] E.S. Basheva, P.A. Kralchevsky, K.D. Danov, S.D. Stoyanov, T.B.J. Blijdenstein, E.G. Pelan, A. Lips, Self-assembled bilayers from the protein HFBII hydrophobin: nature of the adhesion energy, Langmuir 27 (2011) 4481–4488.
[16] R.D. Stanimirova, T.G. Gurkov, P.A. Kralchevsky, K.T. Balashev, S.D. Stoyanov, E.G. Pelan, Surface pressure and elasticity of hydrophobin HFBII layers on the air–water interface: rheology vs structure detected by AFM imaging, Langmuir 29 (2013) 6053–6067.
[17] X.L. Zhang, J. Penfold, R.K. Thomas, I.M. Tucker, J.T. Petkov, J. Bent, A. Cox, I. Grillo, Self-assembly of hydrophobin and hydrophobin/surfactant mixtures in aqueous solution, Langmuir 27 (2011) 10514–10522.
[18] X.L. Zhang, J. Penfold, R.K. Thomas, I.M. Tucker, J.T. Petkov, J. Bent, A. Cox, R.A. Campbell, Adsorption behavior of hydrophobin and hydrophobin/surfactant mixtures at the air–water interface, Langmuir 27 (2011) 11316–11323.
[19] A.R. Mackie, A.P. Gunning, P.J. Wilde, V.J. Morris, Competitive displacement of β-lactoglobulin from the air/water interface by sodium dodecyl sulfate, Langmuir 16 (2000) 8176–8181.
[20] P.A. Gunning, A.R. Mackie, A.P. Gunning, N.C. Woodward, P.J. Wilde, V.J. Morris, Effect of surfactant type on surfactant–protein interactions at the air–water interface, Biomacromolecules 5 (2004) 984–991.
[21] A.R. Mackie, A.P. Gunning, L.A. Pugnaloni, E. Dickinson, P.J. Wilde, V.J. Morris, Growth of surfactant domains in protein films, Langmuir 19 (2003) 6032–6038.
[22] J. Maldonado-Valderrama, A. Martín-Molina, A. Martín-Rodriguez, M.A. Cabrerizo-Vílchez, M.J. Gálvez-Ruiz, D. Langevin, Surface properties and foam stability of protein/surfactant mixtures: theory and experiment, J. Phys. Chem. C 111 (2007) 2715–2723.
[23] B.A. Noskov, O.Yu. Milyaeva, S.-Y. Lin, G. Loglio, R. Miller, Dynamic properties of β-casein/surfactant adsorption layers, Colloids Surf. A 413 (2012) 84–91.
[24] A. Dan, G. Gochev, J. Krägel, E.V. Aksenenko, V.B. Fainerman, R. Miller, Interfacial rheology of mixed layers of food proteins and surfactants, Curr. Opin. Colloid Interface Sci. 18 (2013) 302–310.
[25] F. Ravera, M. Ferrari, E. Santini, L. Liggieri, Influence of surface processes on the dilational visco-elasticity of surfactant solutions, Adv. Colloid Interface Sci. 117 (2005) 75–100.
[26] F. Ravera, G. Loglio, V.I. Kovalchuk, Interfacial dilational rheology by oscillating bubble/drop methods, Curr. Opin. Colloid Interface Sci. 15 (2010) 217–228.
[27] J. Maldonado-Valderrama, J.M. Rodríguez Patino, Interfacial rheology of protein–surfactant mixtures, Curr. Opin. Colloid Interface Sci. 15 (2010) 271–282.
[28] A.A. Mikhailovskaya, B.A. Noskov, S.-Y. Lin, G. Loglio, R. Miller, Formation of protein/surfactant adsorption layer at the air/water interface as studied by dilational surface rheology, J. Phys. Chem. B 115 (2011) 9971–9979.
[29] H.A. Wege, J.A. Holgado-Terriza, A.W. Neumann, M.A. Cabrerizo-Vílchez, Axisymmetric drop shape analysis as penetration film balance applied at liquid–liquid interfaces, Colloids Surf. A 156 (1999) 509–517.
[30] Cs. Kotsmár, D.O. Grigoriev, A.V. Makievski, J.K. Ferri, J. Krägel, R. Miller, H. Möhwald, Drop profile analysis tensiometry with drop bulk exchange to study the sequential and simultaneous adsorption of a mixed β-casein/C12DMPO system, Colloid Polym. Sci. 286 (2008) 1071–1077.
[31] T.F. Svitova, M.J. Wetherbee, C.J. Radke, Dynamics of surfactant sorption at the air/water interface: continuous-flow tensiometry, J. Colloid Interface Sci. 261 (2003) 170–179.
[32] K.G. Marinova, R.D. Stanimirova, M.T. Georgiev, N.A. Alexandrov, E.S. Basheva, P.A. Kralchevsky, Co-adsorption of the proteins β-casein and BSA in relation to the stability of thin liquid films and foams, in: P. Kralchevsky, R. Miller, F. Ravera (Eds.), Colloid and Interface Chemistry for Nanotechnology, CRC Press, Boca Raton, FL, 2013, pp. 439–458, http://dx.doi.org/10.1201/b15262-22.
[33] R. Miller, V.B. Fainerman, M.E. Leser, M. Michel, Kinetics of adsorption of proteins and surfactants, Curr. Opin. Colloid Interface Sci. 9 (2004) 350–356.
[34] S.C. Russev, N. Alexandrov, K.G. Marinova, K.D. Danov, N.D. Denkov, L. Lyutov, V. Vulchev, C. Bilke-Krause, Instrument and methods for surface dilatational rheology measurements, Rev. Sci. Instrum. 79 (2008) 104102.
[35] A. Sheludko, Thin liquid films, Adv. Colloid Interface Sci. 1 (1967) 391–464.
[36] P.A. Wierenga, E.S. Basheva, N.D. Denkov, Modified capillary cell for foam film studies allowing exchange of the film-forming liquid, Langmuir 25 (2009) 6035–6039.
[37] J.T. Petkov, T.D. Gurkov, B.E. Campbell, R.P. Borwankar, Dilatational and shear elasticity of gel-like protein layers on air/water interface, Langmuir 16 (2000) 3703–3711.
[38] A.F.H. Ward, L. Tordai, Time dependence of boundary tensions of solutions: I. The role of diffusion in time effects, J. Chem. Phys. 14 (1946) 453–461.
[39] P. Joos, Dynamic Surface Phenomena, VSP, Utrecht, The Netherlands, 1999.
[40] Cs. Kotsmar, E.V. Aksenenko, V.B. Fainerman, V. Pradines, J. Krägel, R. Miller, Equilibrium and dynamics of adsorption of mixed β-casein/surfactant solutions at the water/hexane interface, Colloids Surf. A 354 (2010) 210–217.
[41] V. Pradines, V.B. Fainerman, E.V. Aksenenko, J. Krägel, R. Wüstneck, R. Miller, Adsorption of protein–surfactant complexes at the water/oil interface, Langmuir 27 (2011) 965–971.
[42] R. Wüstneck, V.B. Fainerman, E.V. Aksenenko, Cs. Kotsmar, V. Pradines, J. Krägel, R. Miller, Surface dilatational behavior of β-casein at the solution/air interface at different pH values, Colloids Surf. A 404 (2012) 17–24.
[43] G. Gochev, I. Retzlaff, E.V. Aksenenko, V.B. Fainerman, R. Miller, Adsorption isotherm and equation of state for β-lactoglobulin layers at the air/water surface, Colloids Surf. A 422 (2013) 33–38.
[44] A. Dan, R. Wüstneck, J. Krägel, E.V. Aksenenko, V.B. Fainerman, R. Miller, Interfacial adsorption and rheological behavior of β-casein at the water/hexane interface at different pH, Food Hydrocolloids 34 (2014) 193–201.
[45] P.A. Kralchevsky, K.D. Danov, G. Broze, A. Mehreteab, Thermodynamics of ionic surfactant adsorption with account for the counterion binding: effect of salts of various valency, Langmuir 15 (1999) 2351–2365.
[46] D.S. Valkovska, G.C. Shearman, C.D. Bain, R.C. Darton, J. Eastoe, Adsorption of ionic surfactants at an expanding air–water interface, Langmuir 20 (2004) 4436–4445.
[47] P.A. Kralchevsky, K.D. Danov, V.L. Kolev, G. Broze, A. Mehreteab, Effect of nonionic admixtures on the adsorption of ionic surfactants at fluid interfaces: 1. Sodium dodecyl sulfate and dodecanol, Langmuir 19 (2003) 5004–5018.
[48] K.D. Danov, P.A. Kralchevsky, The standard free energy of surfactant adsorption at air/water and oil/water interfaces: theoretical vs. empirical approaches, Colloid J. 74 (2012) 172–185.
[49] E.H. Lucassen-Reynders, J. Benjamins, V.B. Fainerman, Dilational rheology of protein films adsorbed at fluid interfaces, Curr. Opin. Colloid Interface Sci. 15 (2010) 264–270.
[50] A.J. Mendoza, E. Guzmán, F. Martínez-Pedrero, H. Ritacco, R.G. Rubio, F. Ortega, V.M. Starov, R. Miller, Particle laden fluid interfaces: dynamics and interfacial rheology, Adv. Colloid Interface Sci. 206 (2014) 303–319.
[51] K. Ahnert, M. Abel, Numerical differentiation of experimental data: local versus global methods, Comput. Phys. Commun. 177 (2007) 764–774.
[52] B.A. Noskov, A.V. Latnikova, S.-Y. Lin, G. Loglio, R. Miller, Dynamic surface elasticity of β-casein solutions during adsorption, J. Phys. Chem. C 111 (2007) 16895–16901.
[53] A. Hambardzumyan, V. Aguie-Beghin, M. Daoud, R. Douillard, β-Casein and symmetrical triblock copolymer (PEO–PPO–PEO and PPO–PEO–PPO) surface properties at the air–water interface, Langmuir 20 (2004) 756–763.